

14. SITE 1163¹

Shipboard Scientific Party²

PRINCIPAL RESULTS

Site 1163 is located in Segment B4, 188 km west of Site 1162. The sea-floor magnetic age in this area is ~17 Ma, ~1 m.y. younger than at Sites 1162 and 1164. The site is located in a shallow sediment-filled valley between two apparently uplifted blocks on the western flank of the 126°E fracture zone that separates Segment B4 from Segment B5 and marks the present-day boundary between Pacific- and Indian-type mantle domains at the Southeast Indian Ridge (SEIR). This site lies on a ±1-m.y. time line along with Sites 1164 (Segment B5) and 1162 (Zone A). This site placement was designed to test the distribution of Pacific- and Indian-type mantle across the three zones at 17–18 Ma.

Hole 1163A was spudded in 4354 m water depth and was washed through ~161 m of sediment, from which we recovered 2.1 m of variably colored carbonate-rich clay. Rotary drilling continued the hole 47.1 m into volcanic basement; we recovered 15.7 m (33%) of moderately plagioclase-olivine phyric pillow basalt (Unit 1) and aphyric pillow basalt (Unit 2). Calcareous, clay-cemented hyaloclastite breccia and calcarenite were also present as interpillow fill in Unit 2. Carbonate-, clay-, and Mn oxide-filled fractures also contain lithic fragments of basalt and palagonite. Low-temperature alteration to Fe oxyhydroxide and clay is generally confined to narrow alteration halos along fractures, veins, and exterior surfaces.

One basalt glass and one whole rock were selected from each hole for major and trace element analyses. Glasses were analyzed by shipboard inductively coupled plasma-atomic emission spectrometry (ICP-AES), whereas whole rocks were analyzed by X-ray fluorescence (XRF) only. The glasses are both primitive, with ~9.0 wt% MgO, and, as at most other sites, the whole rocks have 0.5–1.0 wt% less MgO than the glasses. Trace element, and possibly major element, concentrations vary widely at constant MgO, expanding the known range of the inherently

¹Examples of how to reference the whole or part of this volume.

²Shipboard Scientific Party addresses.

highly variable Segment B4 lava population and suggesting that this variability (the hallmark of 0- to 5-Ma Segment B4 lavas) is a long-lived feature associated with the axis of the depth anomaly. Ba and Zr systematics of the glasses indicate that Indian-type mantle was present beneath Segment B4 ~17 m.y. ago.

OPERATIONS

Transit to Site 1163

The west-northwest transit from Site 1162 to Site 1163 took about 10 hr at an average speed of 10.4 kt. At 2330 hr on 31 December, we slowed to 5 kt and ran a south-to-north single-channel seismic (SCS) survey on a line 1 nmi west of and parallel to the precruise site survey track. Since the valley hosting the sediment-filled pond (our proposed site) opened to the west, we hoped that we would find a more inviting drilling target along this line. When we could find no suitable sediment cover along this survey track, we steered a southeasterly heading, which carried us directly over the Global Positioning System (GPS) coordinates of the prospectus site. Although the sediment pond is a small target at this location, we decided that the sediment thickness was sufficient to provide lateral support for the bottom-hole assembly (BHA). Although the duration of the survey was only 1.6 hr and covered 8 nmi, it had the distinction of lasting from one millennium to the next.

Hole 1163A

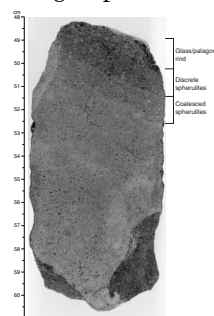
The precision depth recorder (PDR) water depth referenced to the dual-elevator stool at this site is 4365.4 m. The nine-collar BHA employed at the other sites was reassembled, along with a previously used hard-formation C-7 four-cone rotary bit that was still in good condition. This bit was run with a mechanical bit release. We began Hole 1163A at 1030 on 1 January by washing through ~160 m of sediment below seafloor at an average penetration rate of 54 m/hr. When the driller noted a hard contact, we pulled the wash barrel (Core 187-1163A-1W, 0.0 to 161.0 meters below seafloor [mbsf]; Table T1). We advanced Hole 1163A by rotary coring 161.0–208.1 mbsf (Cores 187-1163A-2R to 11R) with generally good drilling conditions and 33% recovery. Microsphere tracers were deployed on Core 187-1163A-2R. We terminated operations at this site when we reached our depth objective of ~50 mbsf. The drill string cleared the seafloor at 2345 hr on 2 January and the rotary table at 0700 hr on 3 January.

IGNEOUS PETROLOGY

Hole 1163A was rotary cored into igneous basement from 161 to 208.1 mbsf, and we recovered 15.7 m of core, which is 33.3% recovery (Cores 187-1163A-2R through 11R). Lavas from this hole were assigned to two lithologic units. Unit 1 (Section 187-1163A-2R-1 through Section 3R-1 [Piece 14]) is a medium gray, moderately plagioclase-olivine phyric basalt. Unit 2 (Sections 187-1163A-3R-1 [Piece 15] through 11R-2) is a medium gray aphyric basalt. We interpret this hole as having sampled intact pillow lavas, based on the high percentage of pieces with arcuate chilled margins (57 of 265 basalt pieces, equal to 21.5%) (Fig. F1) and

T1. Coring summary, Site 1163, p. 31.

F1. Pillow lava fragment showing chilled margin, p. 9.



on the presence of radial fractures. Pillows from Unit 2 are larger than most pillows encountered earlier on this leg, based on the lengths of individual pieces (as long as 70 cm) (Section 187-1163A-9R-1 [Piece 9]).

Ten pieces of interpillow sediment are interspersed with Unit 2 basalts in Sections 187-1163A-5R-2 through 11R-2. They range from clayey calcarenite to calcareous, clay-cemented hyaloclastite breccia (Fig. F2). Similar sediment is also present as patchy coatings up to several millimeters thick on the outsides of some basalt pieces (Fig. F3).

Unit 1

Unit 1 is a slightly to moderately altered (see “Alteration,” p. 4) medium gray, plagioclase-olivine phyric basalt. Phenocrysts include 1%–2% euhedral to subhedral equant olivine (as large as 4 mm) and 2% subhedral prismatic to tabular plagioclase (as large as 5 mm). Plagioclase is commonly twinned with some of the larger phenocrysts displaying discontinuous zoning and sieve-textured cores. Approximately 15% (in Sections 187-1163A-2R-1 and 2) to 25% (in Section 3R-1) of phenocrysts are included in glomerocrysts made up of several small (~1 mm) prismatic plagioclase and/or equant olivine grains (Fig. F4).

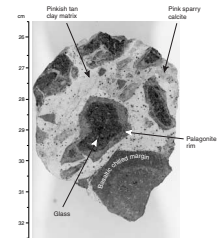
Eight pieces (i.e., 17% of the pieces recovered) have chilled margins ± glass/palagonite rinds ranging from <1 to 7 mm thick (e.g., Section 187-1163A-3R-1 [Piece 3]). Inward from these rinds, a zone of discrete spherulites as wide as 3 mm (e.g., Section 187-1163A-3R-1 [Piece 3]) is followed by a zone of coalesced spherulites as wide as 1.5 cm (e.g., Section 187-1163A-2R-1 [Piece 5]) before the more crystalline interior of the pillow is reached. Vesicles (<1%) are present in only three pieces (e.g., Section 187-1163A-2R-2 [Piece 3]). These are spherical, ~0.3 mm in diameter, and lined with either bluish gray cryptocrystalline silica or light gray clay.

The microcrystalline groundmass texture is intersertal, dominated by ~50% mesostasis with ~40% plagioclase and ~2% each of olivine, clinopyroxene, and opaque minerals. The plagioclase is seriate and ranges from sheaf quench textures to lath-shaped microphenocrysts as long as ~1 mm. Olivine is also seriate and ranges from quench morphologies to equant skeletal microphenocrysts as large as ~1 mm. Olivine seldom occurs as discrete crystals in the groundmass but rather in association with groundmass plagioclase. Clinopyroxene ranges from plumose quench texture in the groundmass to euhedral elongate crystals as long as 0.25 mm in miarolitic cavities. The opaque minerals are generally small (~2 μm in diameter) and spherical but may be as large as 30 μm in diameter in miarolitic cavities. Cr spinel (as large as 0.3 mm) is present in trace amounts and as inclusions in several olivine phenocrysts (e.g., Section 187-1163A-2R-2, Piece 3).

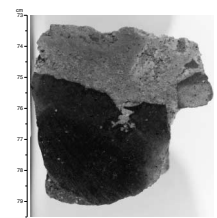
Unit 2

Unit 2 is a slightly to moderately altered (see “Alteration,” p. 4) medium gray aphyric basalt. Prismatic plagioclase phenocrysts as long as 3 mm are present throughout the unit but are rare (e.g., Section 187-1163A-5R-2 [Piece 8]). Chilled margins ± glass/palagonite rinds occur on 49 pieces (i.e., 22.4% of the pieces recovered). These rinds range from <1 to 8 mm thick (e.g., Section 187-1163A-7R-2 [Piece 1B]) and commonly contain plagioclase microlites. Inward from these rinds, a zone of discrete spherulites as wide as 4 mm (e.g., Section 187-1163A-11R-2 [Piece 4]) is followed by a zone of coalesced spherulites as wide as

F2. A calcareous clay-cemented hyaloclastite breccia from Unit 2, p. 10.



F3. Sediment attached to the outer surface of aphyric basalt (Unit 2), p. 11.



F4. Plagioclase + olivine glomerocryst, p. 12.



5 mm (e.g., Section 187-1163A-5R-1 [Piece 3]) before the more crystalline interior is reached. The unit contains ~2% spherical vesicles, on average 0.3 mm in diameter, with variable filling (see “Alteration,” p. 4) and ~3% miarolitic cavities (as large as 0.8 mm across) with euhedral elongate clinopyroxene (as large as 0.1 mm).

The microcrystalline groundmass texture is intersertal, dominated by ~35% each of mesostasis and plagioclase. Plagioclase ranges from sheaf quench textured (Fig. F5) to prismatic microphenocrysts on average 0.6 mm long (but as large as 1.5 mm). Clinopyroxene (~20%) occurs mainly as plumose quench textures (Fig. F6), except in miarolitic cavities, where it forms euhedral elongate crystals as long as 0.1 mm (Fig. F7). The remaining groundmass consists of ~5% skeletal to equant olivine as large as 1 mm and <1% opaque minerals. The opaque minerals are generally small (~2 µm in diameter) and spherical. The larger, lath-shaped plagioclase and skeletal olivine (~30% of the crystals) are microphenocrysts that commonly form glomerocrysts (Fig. F8).

Sediment and Breccia

Ten pieces of sediment that range from pinkish tan clayey calcarenite with pink sparry calcite (e.g., Section 187-1163A-7R-1 [Piece 3]) to pinkish tan calcareous clay-cemented hyaloclastite breccia (e.g., Section 187-1163A-8R-1 [Piece 5]) were recovered along with the basalt of Unit 2. The breccia is poorly sorted with ~50% angular to subangular clasts of basaltic chilled margins and glass/palagonite rind fragments that range in size from 1 mm to 4.5 cm. The glass/palagonite fragments commonly contain microlites of plagioclase, similar to the pillow rinds in the Unit 2 aphyric basalt, suggesting that the fragments were derived from the pillows. The glass fragments also have concentric rims of palagonite, indicating that this alteration occurred within the sediment. Thirty-eight pieces of aphyric basalt from Unit 2 have patchy coatings of similar sediment, ranging in thickness from <1 mm (e.g., Section 187-1163A-7R-2 [Piece 5]) to 2.2 cm (e.g., Section 187-1163A-6R-1 [Piece 9]).

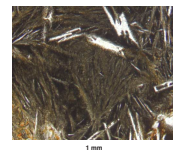
ALTERATION

Basalts recovered from Hole 1163A are divided into two lithologic units. Both units have undergone slight to moderate low-temperature alteration. In slightly altered pieces, alteration is generally confined to narrow halos along fractures, veins, and exterior surfaces; many pieces have fresh interiors. In moderately altered pieces, alteration is more pervasive, which is mostly due to increased vein density and slightly wider alteration halos (e.g., Sections 187-1163A-6R-1 and 2).

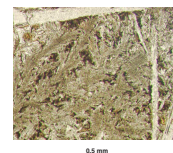
Calcareous sediment with Mn oxide spots and lithic clasts of basalt and/or partially to completely altered glass is present as single pieces (Fig. F9) or attached to basalt pieces (Fig. F10) in several sections. The palagonite around glass fragments is concentric, suggesting that alteration took place within the sediment.

Fractures, unfilled or lined with Fe oxyhydroxide or/and Mn oxide, are present in basalt pieces throughout the core (Fig. F11). In some places, thin (<0.2–0.25 mm wide) veins filled with white clay and cryptocrystalline silica (e.g., Section 187-1163A-3R-2, [Piece 1]), quartz, and Mn oxide (Section 187-1163A-5R-2 [Piece 12]), or red silica and clay (Section 187-1163A-10R-2 [Piece 5]) are present. Veins (0.2–10 mm

F5. Plagioclase sheaf quench texture in aphyric basalt (Unit 2), p. 13.



F6. Clinopyroxene plumose quench texture (Unit 2), p. 14.



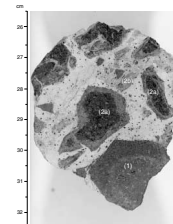
F7. Miarolitic cavity in aphyric basalt, p. 15.



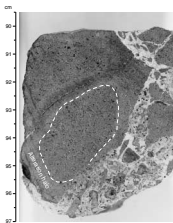
F8. Groundmass olivine + plagioclase glomerocryst, p. 16.



F9. Calcite-cemented basaltic breccia with clasts of basalt and basaltic glass, p. 17.



F10. Calcite-cemented basalt that was altered before brecciation, p. 18.



wide) filled with cream-colored carbonate and/or clay \pm Mn oxide are common in most sections (Figs. F12, F13). The carbonate includes both micritic and sparry calcite (Fig. F14). Larger micritic veins commonly also contain 5%–20% lithic fragments of basalt and palagonite (Fig. F13) probably derived from the host pillow basalt, implying transport of sediment (similar to sediment attached to outer surfaces of basalt pieces) into the veins. Sparry calcite varies from predominantly pinkish brown to white. White sparry calcite crosscuts both the micrite and the pinkish brown sparry calcite, whereas the pinkish brown sparry calcite only cuts through the micrite. The sparry calcite may, to some extent, have been derived from the micrite by recrystallization. Mn oxide is present in all types of calcite but is most common in the micrite. Locally, vein boundaries are lined with Mn oxide and/or Fe oxyhydroxide.

Alteration is mostly restricted to oxidation halos, paralleling fractures, veins, and outer margins of pieces (Figs. F12, F13, F15). In slightly altered pieces, the alteration halos are narrow (3–5 mm) (Fig. F13). In moderately altered pieces, the vein density is higher, and the halos are generally wider (up to 10 mm). The halo width may vary along a single vein, as in Section 187-1163A-6R-1 (Piece 7E), where it changes from 0 to 7 mm over a distance of a few centimeters. Rarely, 2- to 4-cm-wide halos are developed along outer margins of pieces (e.g., Section 187-1163A-2R-2 [Piece 10] and 8R-1 [Piece 1]). Some pieces have concentric zoned alteration halos that change from dark orange-brown to brown in the outermost zone to a lighter brown zone and, finally, to a darker gray inner zone adjacent to the lighter gray fresh interior (e.g., Section 187-1163A-3R-1 [Piece 1] and 9R-1 [Piece 9]).

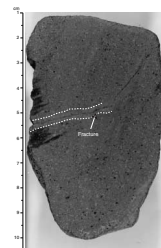
Within the alteration halos, 50%–100% of olivine is replaced by Fe oxyhydroxide and clay. Plagioclase is usually unaltered. In moderately but pervasively altered pieces, the alteration involves replacement of olivine and groundmass by Fe oxyhydroxide + clay \pm calcite. Vesicles are unfilled to variably filled with clay or calcite or lined with blue cryptocrystalline silica and clay \pm Fe oxyhydroxide \pm Mn oxide. In some places, cavities are lined with blue cryptocrystalline silica and clay or calcite. Glassy pillow margins were recovered in most cores, and these are altered on the outer surfaces to yellowish brown to orange palagonite.

MICROBIOLOGY

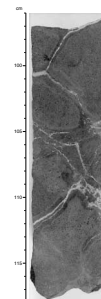
Four rock samples were collected as soon as the core liners were split at Site 1163 to characterize the microbial community inhabiting this environment (Table T2). One breccia fragment (Sample 187-1163A-8R-1 [Piece 4, 33–35 cm]), two pillow basalt fragments composed of partially altered glass rinds and crystalline basalt (Samples 187-1163A-2R-1 [Piece 5, 27–29 cm] and 4R-1 [Piece 9, 50–52 cm]), and one fragment of crystalline basalt (Sample 187-1163B-10R-1 [Piece 5, 62–65 cm]) (see “Igneous Petrology,” p. 2) were sampled. To sterilize them, the outer surfaces of the rocks were quickly flamed with an acetylene torch, and enrichment cultures and samples for DNA analysis and electron microscope studies were prepared (see “Igneous Rocks,” p. 7, in “Microbiology” in the “Explanatory Notes” chapter).

Fluorescent microsphere tests were carried out for one core to evaluate the extent of contamination caused by drilling fluid (see “Tracer Test,” p. 9, in “Microbiology” in the “Explanatory Notes” chapter and Table T2). Pieces of rock were rinsed in nanopure water, and the water

F11. Fracture with minor alteration halo cutting basalt, p. 19.



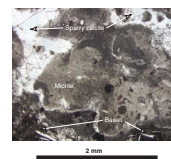
F12. Calcite veins cutting basalt and surrounded by alteration halos, p. 20.



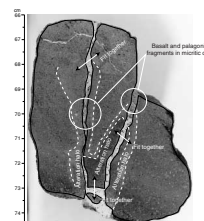
F13. Carbonate veins surrounded by alteration halos in basalt, p. 21.



F14. Sparry calcite vein cutting micritic calcite and basalt, p. 22.



F15. Aphyric basalt piece with alteration halos along the outer margins, p. 23.



was then filtered. Thin sections were examined to determine the extent of contamination inside the samples. Filters and thin sections were examined under a fluorescence microscope for the presence of microspheres. Microspheres were detected on the filter. In the thin sections, microspheres were located both inside fractures and on thin-section surfaces. The microspheres on the polished surfaces were always found close to fractures or to thin-section (i.e., piece) margins and may have been relocated by polishing. Nineteen microspheres were observed in thin sections from Core 187-1163A-2R.

STRUCTURAL GEOLOGY

Fractures and veins are the principal structures developed in basalts from Hole 1163A. Veins are filled by cream-colored micritic carbonate and/or clay, pinkish brown finely crystalline sparry calcite, and white sparry calcite (see Fig. F16 and “Alteration,” p. 4). The cream-colored micritic carbonate and/or clay appears to be derived from interpillow sediments. Therefore, most veins are considered to represent sediment-filled open fractures.

Fractures and veins are abundant in the lower part of Hole 1163A (Fig. F17). A plot of fracture + vein density (Fig. F17) on a section-by-section basis indicates a general increase in the abundance of fractures and veins downhole.

Fracture + vein density ranges from 4.5 to 38.5/m and averages 19.0/m (Fig. F17). The vein density ranges from 0 to 28.8/m and averages 11.4/m. The calculated vein volume percent ranges from 0 to 3.4 and averages 1.1.

SITE GEOPHYSICS

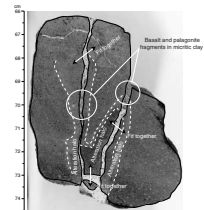
Site selection for Site 1163 was based on a SCS survey conducted during the *R/V Melville* cruise Boomerang 5 in 1996. A 1.6-hr SCS and 3.5-kHz PDR survey was conducted on the approach to Site 1163 (*JOIDES Resolution* [JR] SCS line S11; Fig. F18) to ensure the correct site location by comparing the GPS-navigated SCS data with the previous SCS image and to verify sediment thickness. The water gun was triggered at a shot interval of 12 s, equivalent to ~31 m at 5.1 kt (the ship’s average speed). A 1.5-km-wide basin structure is revealed in this profile between shotpoints 270 and 310 (Fig. F19). Site 1163 is close to the prospectus site AAD-3b (AAD = Australian Antarctic Discordance) at a position corresponding to shotpoint 292 of the seismic profile. Sediment cover was estimated to be from 5.88 to 6.01 s in two-way traveltime, equivalent to at least 130 m (see Fig. F19). We washed through 161 m of sediment in Hole 1163A before basement was reached.

SEDIMENTS

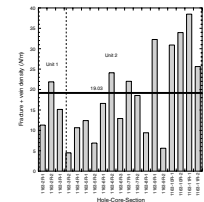
One wash barrel was recovered from Hole 1163A (Core 187-1163A-1W; 0.0–161.0 mbsf). The entire core is clay of varying color, but the boundaries and the thicknesses of these intervals are unknown. All intervals in this core contain abundant carbonate, as evidenced by their reaction with dilute HCl (~5%–10%). From 0 to ~10 cm in Section 187-1163A-1W-1 is a soupy, very light cream-colored ooze. From ~10 to 99

T2. Rock samples for cultures, DNA analysis, SEM/TEM, and contamination studies, p. 32.

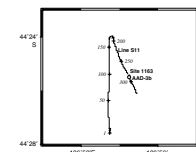
F16. Basalt cut by veins filled by micritic clay, p. 24.



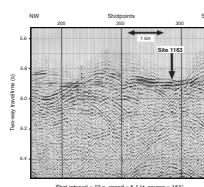
F17. Plot of fracture + vein density, p. 25.



F18. Track chart of the SCS survey line S11, p. 26.



F19. SCS profile of line S11 from shotpoints 175 to 322, p. 27.



cm is a light greenish gray, moderately stiff clay. The upper contact of this interval is severely drilling disturbed and smeared over 15 cm, but the lower contact is sharp and irregular. From 99 to 105 cm is a pale cream clay, and from 105 to 133 cm is a very light brown clay with rare 1- to 3-cm-thick layers and lenses of light brown clay. The contacts of the layers and lenses are sharp and irregular. From 133 to 136 cm is a thin interval of medium brown clay, underlain by an interval of layered, very light brown to medium brown clay. This interval extends through Section 187-1163A-1W-2 to the top 4 cm of the core catcher. The layers range from 1 mm to 3 cm thick and have predominantly sharp but irregular contacts. A few layer contacts are diffuse, but this may be an artifact of the coring or splitting process. From 4 to 13 cm in Section 187-1163A-1W-CC is a medium brown, drilling-disturbed clay. A single fragment of basalt with fresh glass was embedded in a thin (4 cm) interval of severely drilling-disturbed light brown clay at the base of the core catcher.

GEOCHEMISTRY

Introduction

Site 1163 is located on ~17-Ma crust within Segment B4 of the AAD. Two lithologic units are identified in Hole 1163A, based on macroscopic and microscopic examination (see “[Igneous Petrology](#),” p. 2). Two glass samples—one from a pillow basalt fragment (Sample 187-1163A-1W-CC) and one from a glass clast in carbonate-cemented breccia (Sample 187-1163-8R-1, 41–43 cm)—were analyzed for major and trace elements by ICP-AES (Table T3). Three whole-rock powders were analyzed for major and trace elements by XRF only.

Hole 1163A

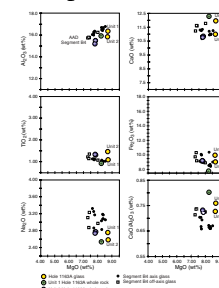
Both Units 1 and 2 basalt glasses from Hole 1163A have ~9.0 wt% MgO; in contrast, whole rocks have 0.5–1.0 wt% less MgO (Fig. F20), as has been observed at previous sites during Leg 187. The glasses and whole rocks overlap in all other major and trace element concentrations, except for Ni, which is noticeably higher in whole-rock samples. Average analyses suggest that Unit 1 and Unit 2 glasses have different major element characteristics, but the ranges reported in Table T3 overlap substantially (Fig. F21), indicating that some differences are analytical. However, analysis of trace elements was less problematic, so we are confident that the trace element difference observed between the Unit 1 and Unit 2 glasses is significant. In particular, Unit 2 is higher in all trace elements except Cr (Fig. F21). Unit 2 also has lower CaO/Al₂O₃ ratios, suggesting a lower degree of melting, consistent with its elevated trace element contents. Unit 1 and Unit 2 whole rocks show the same compositional contrasts as their associated glasses.

Temporal Variations

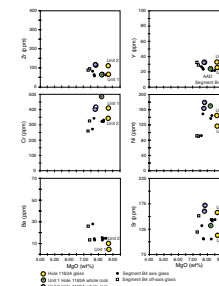
The glasses from Hole 1163A are more primitive (i.e., ~9.0 wt% MgO) than any basalt yet recovered within Segment B4. A hallmark of AAD Segment B4, the present focus of the depth anomaly, is its compositional diversity, driven by variations in mantle melting processes rather than by low-pressure crystal fractionation. Simple data trends with de-

T3. Compositions of basalts from Site 1163, p. 33.

F20. Major element compositions vs. MgO of basalts, Holes 1163A and 1163B, p. 28.



F21. Trace element compositions vs. MgO, Hole 1163A basalts, p. 29.



creasing MgO are rare. This generalization also applies to Site 1163 lavas, which display a relatively large range in trace element concentrations at a given MgO content. Y, Zr, Cr, and TiO₂ contents are higher, and Ba and Na₂O are lower, than in younger Segment B4 lavas, increasing the compositional diversity within this segment beyond that previously documented. The slightly higher CaO/Al₂O₃ ratios and lower Na₂O contents of Site 1163 glasses indicate a higher degree of melting at 17 Ma than beneath the present Segment B4 axis. Higher Y, Zr, and TiO₂ contents also suggest a mantle source higher in these constituents relative to the mantle source for present-day Segment B4 lavas.

Mantle Domain

The Zr/Ba systematics of Site 1163 basalts indicate an Indian- to Transitional Pacific-type mantle source beneath Segment B4 of the AAD at ~17 Ma (Fig. F22A). Both Unit 1 and Unit 2 glasses have higher Zr/Ba ratios and lower Ba contents than present-day Segment B4 lavas and, consequently, plot closer to the Pacific-type field. In spite of plotting within the Pacific field defined by zero-age SEIR basalt glass, the Na₂O/TiO₂ systematics suggest an Indian-type mantle affinity (Fig. F22B) based on the distribution of Leg 187 glass samples. In addition, low Na₂O has been a consistent characteristic of Leg 187 basalts (see **“Sodium and Titanium,”** p. 13, in the **“Leg Summary”** chapter). The lower Na₂O and often higher TiO₂ contents of Site 1163 lavas offset the data to a position below the original division based on 0- to 7-Ma SEIR mid-ocean-ridge basalt (MORB) glass data, even for rocks whose Ba/Zr values give a clear indication of Indian mantle provenance. We believe this indicates a significant contrast in the major and trace element character of the mantle and its melting properties in this region between the time Leg 187 lavas were produced and the present day.

F22. Variations of Zr/Ba vs. Ba and Na₂O/TiO₂ vs. MgO, Site 1163 glass and whole-rock samples, p. 30.

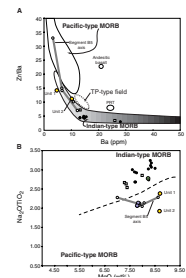


Figure F1. Photograph of Section 187-1163A-8R-1 (Piece 8, 48–61 cm), showing a typical chilled margin sequence from a glassy outer rind to more crystalline pillow lava interior (Unit 2).

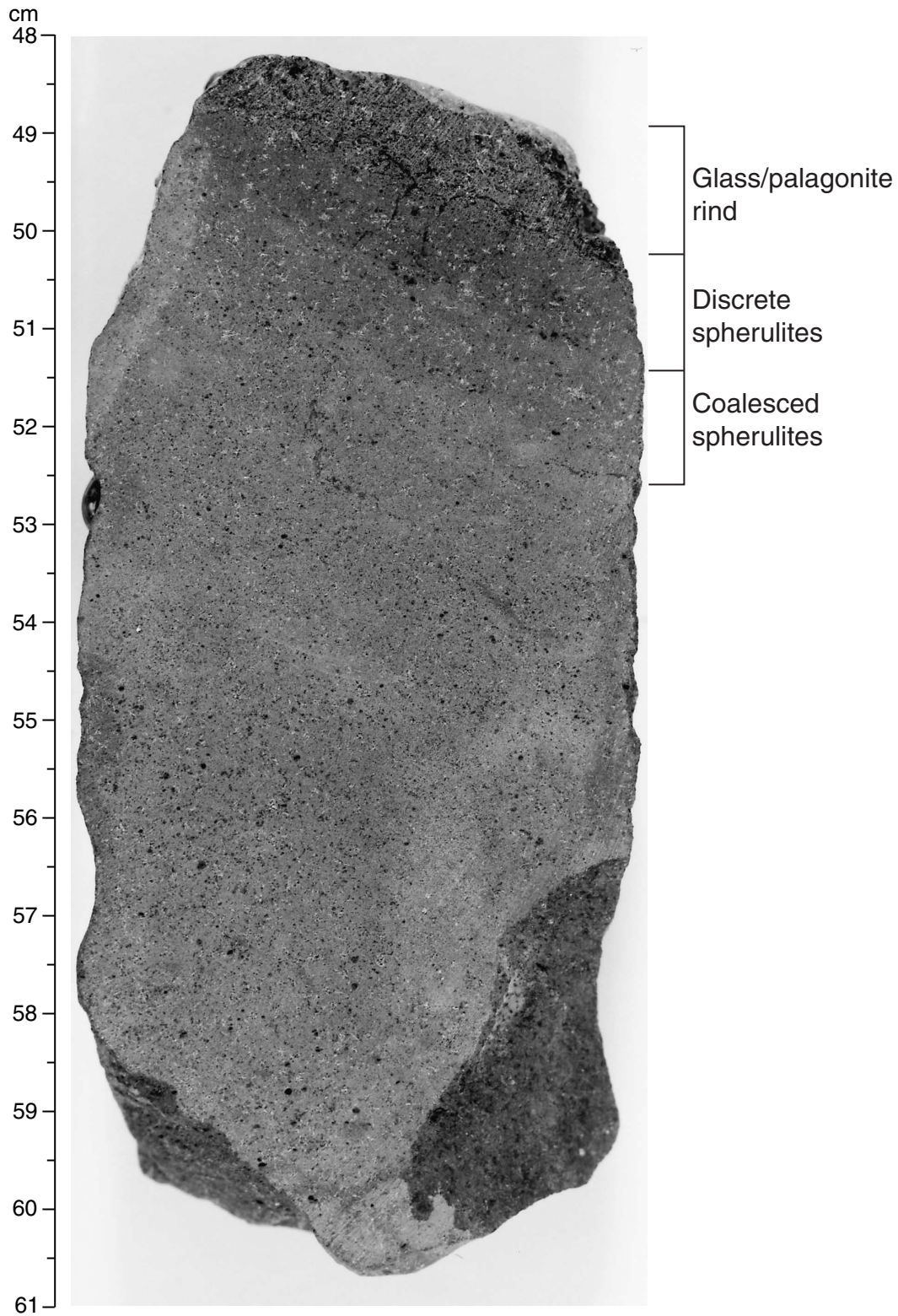


Figure F2. Photograph of Section 187-1163A-7R-2 (Piece 2, 26–32 cm), showing a calcareous-clay cemented hyaloclastite breccia from Unit 2. Notice the concentric palagonite rim around the edge of the glass fragment and the basaltic clast with ~4-mm-wide chilled margin. This basalt clast contains small plagioclase microlites like those seen in the aphyric basalt of Unit 2.

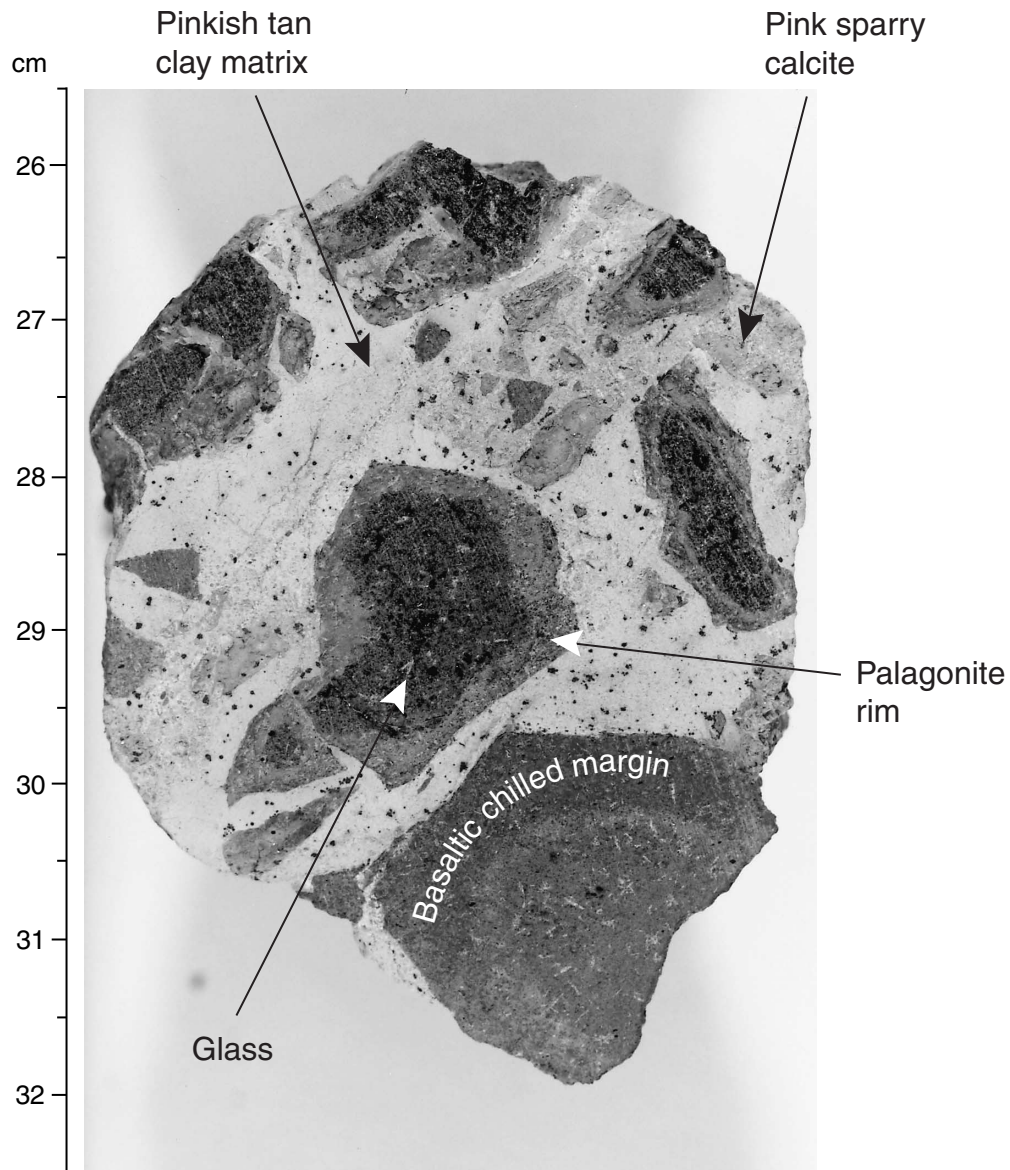


Figure F3. Photograph of Section 187-1163A-6R-1 (Piece 9, 73–79 cm), showing sediment attached to the outer surface of aphyric basalt (Unit 2). Nearest to the basalt, the sediment is stained reddish orange. This staining fades into the sediment's typical pinkish tan color over an ~5-mm-wide interval.

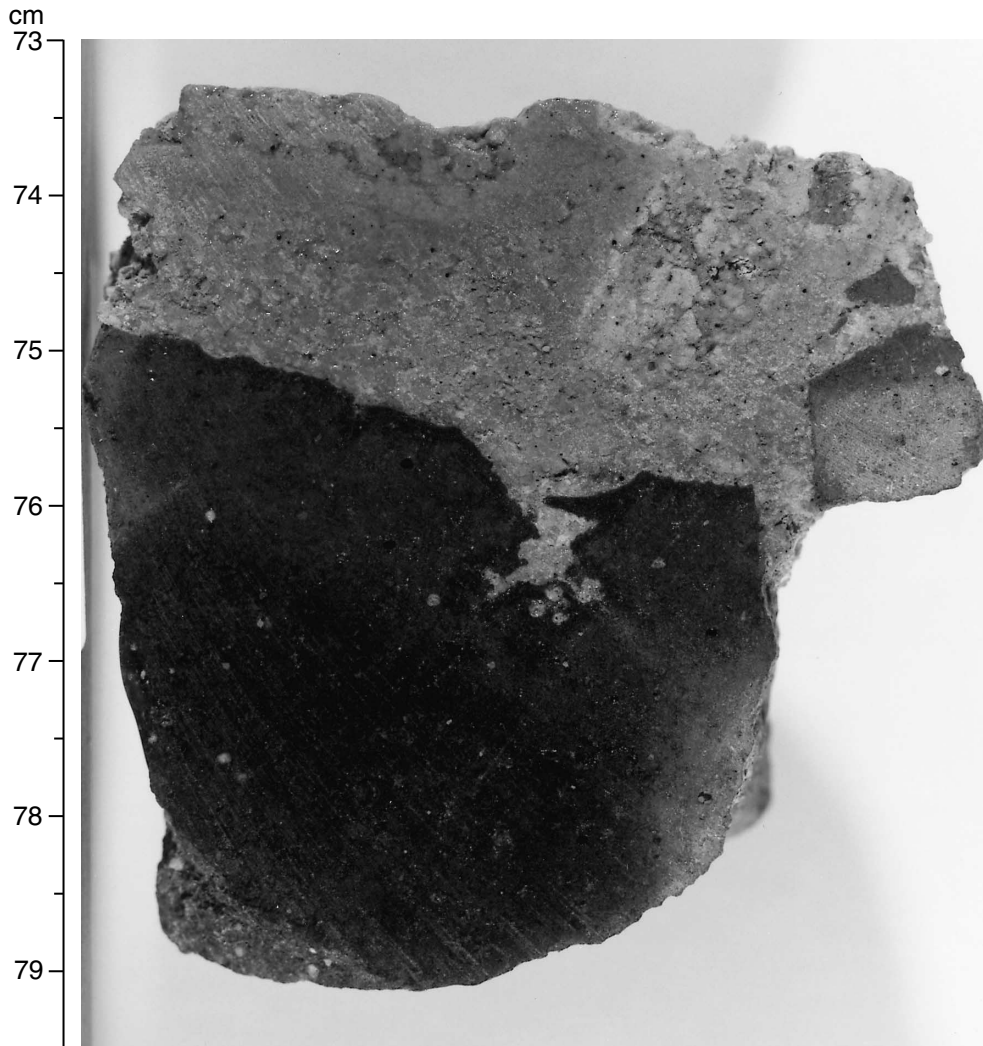
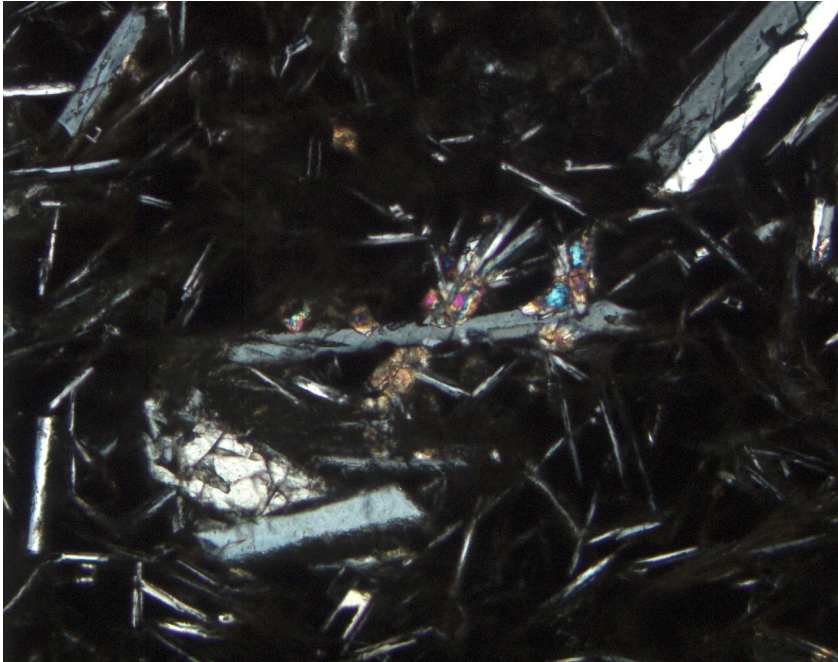


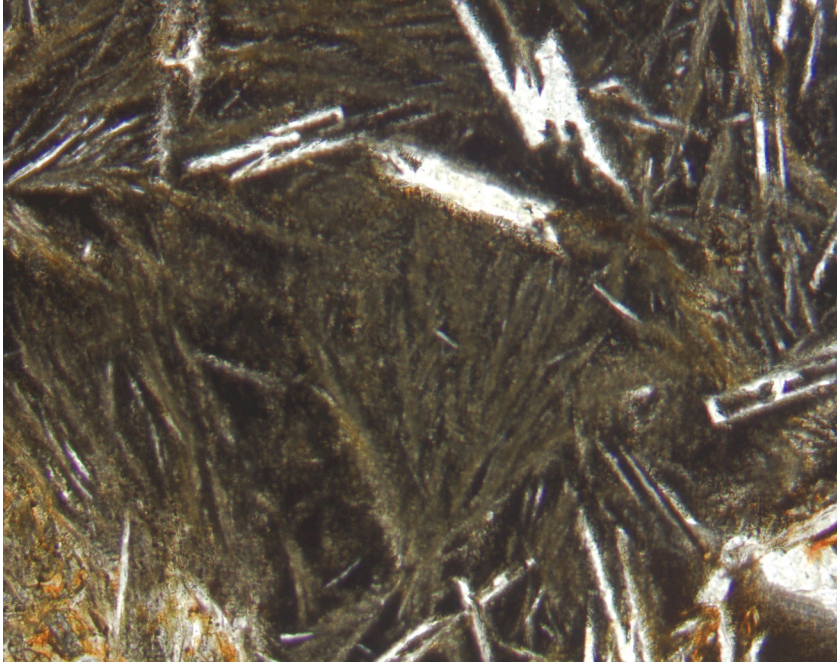
Figure F4. Photomicrograph, with crossed polars, of Sample 187-1163A-2R-1 (Piece 4; see “[Site 1163 Thin Sections](#),” p. 23), showing a glomerocryst of plagioclase and olivine microphenocrysts from Unit 1 basalt.



1 mm



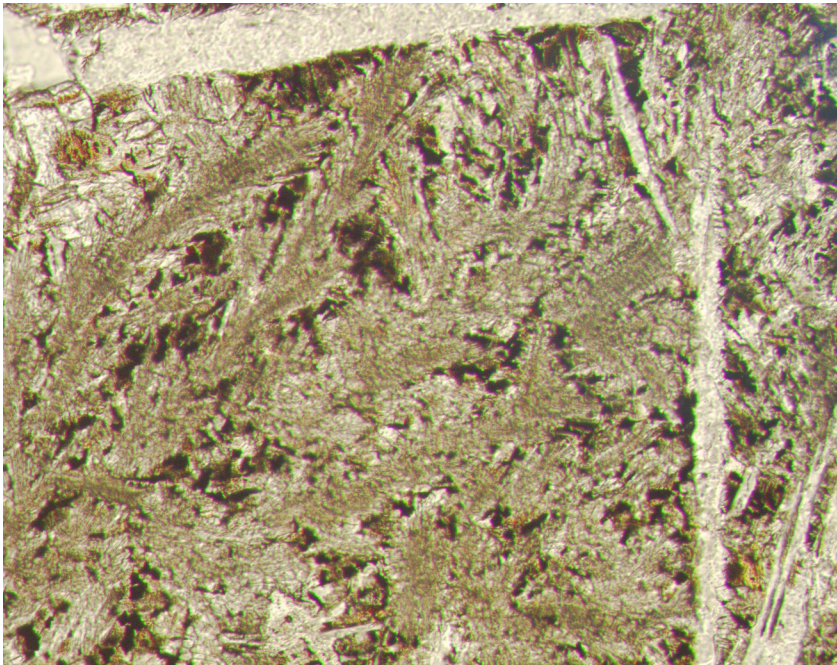
Figure F5. Photomicrograph in plane-polarized light of Sample 187-1163A-3R-2 (Piece 10; see “[Site 1163 Thin Sections](#),” p. 27), showing a plagioclase sheaf quench texture and skeletal plagioclase in the groundmass of aphyric basalt (Unit 2). Notice the Fe oxyhydroxide staining along groundmass plagioclase (lower right corner) and the replacement of groundmass mesostasis by clay and Fe oxyhydroxide (lower left corner).



1 mm



Figure F6. Photomicrograph in plane-polarized light of Sample 187-1163A-3R-2 (Piece 10; see “[Site 1163 Thin Sections](#),” p. 27), showing clinopyroxene plumose quench texture and plagioclase laths in the groundmass of aphyric basalt (Unit 2). The golden brown (upper left corner) is clay replacing mesostasis.



0.5 mm

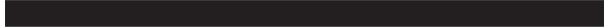


Figure F7. Photomicrograph in plane-polarized light of Sample 187-1163A-3R-2 (Piece 10; see “[Site 1163 Thin Sections](#),” p. 27), showing clay-filled miarolitic cavity in aphyric basalt with larger euhedral elongate clinopyroxene.

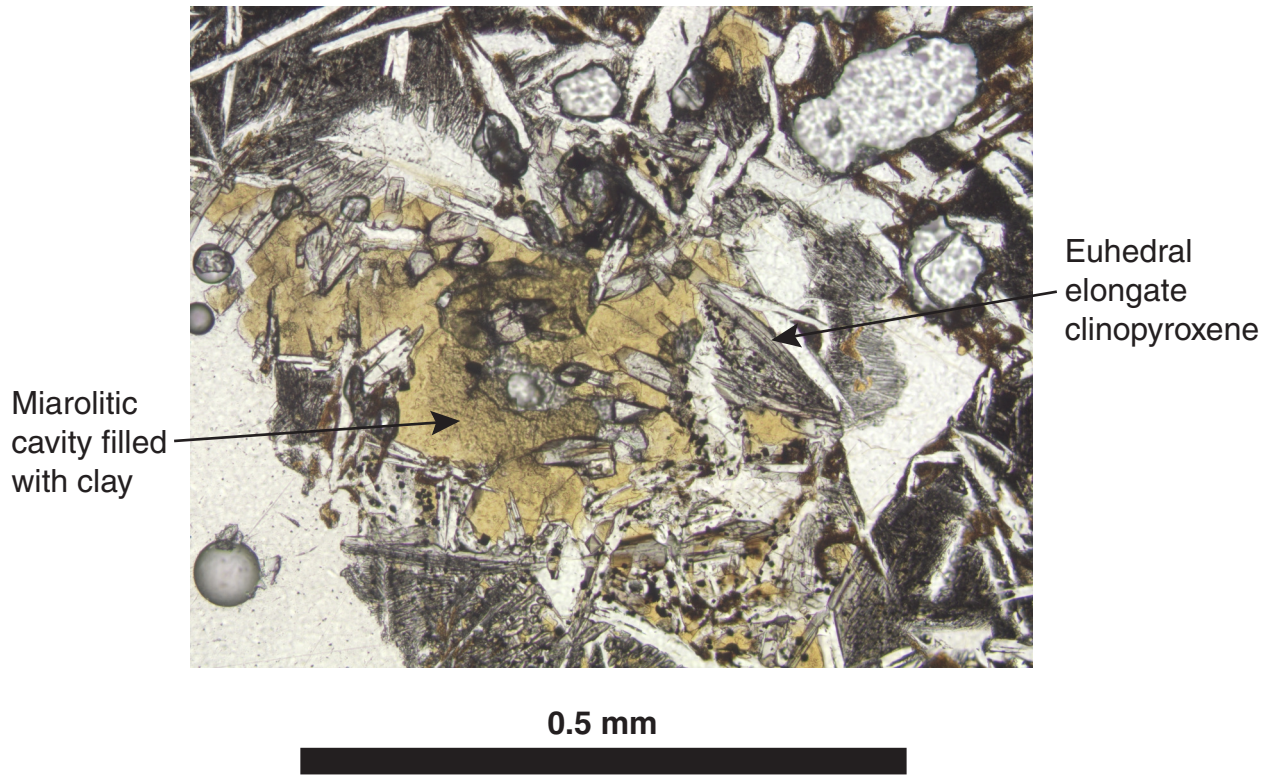


Figure F8. Photomicrograph, with crossed polars, of Sample 187-1163A-10R-1 (Piece 13; see “[Site 1163 Thin Sections](#),” p. 30), showing a glomerocryst of olivine and plagioclase in aphyric basalt from Unit 2.



1 mm



Figure F9. Photograph of interval 187-1163A-7R-2, 26-32 cm, showing a calcite-cemented basaltic breccia that contains clasts of basalt with (1) altered margins and (2) glassy margins: (2a) partially to (2b) completely altered to concentric layers of palagonite.

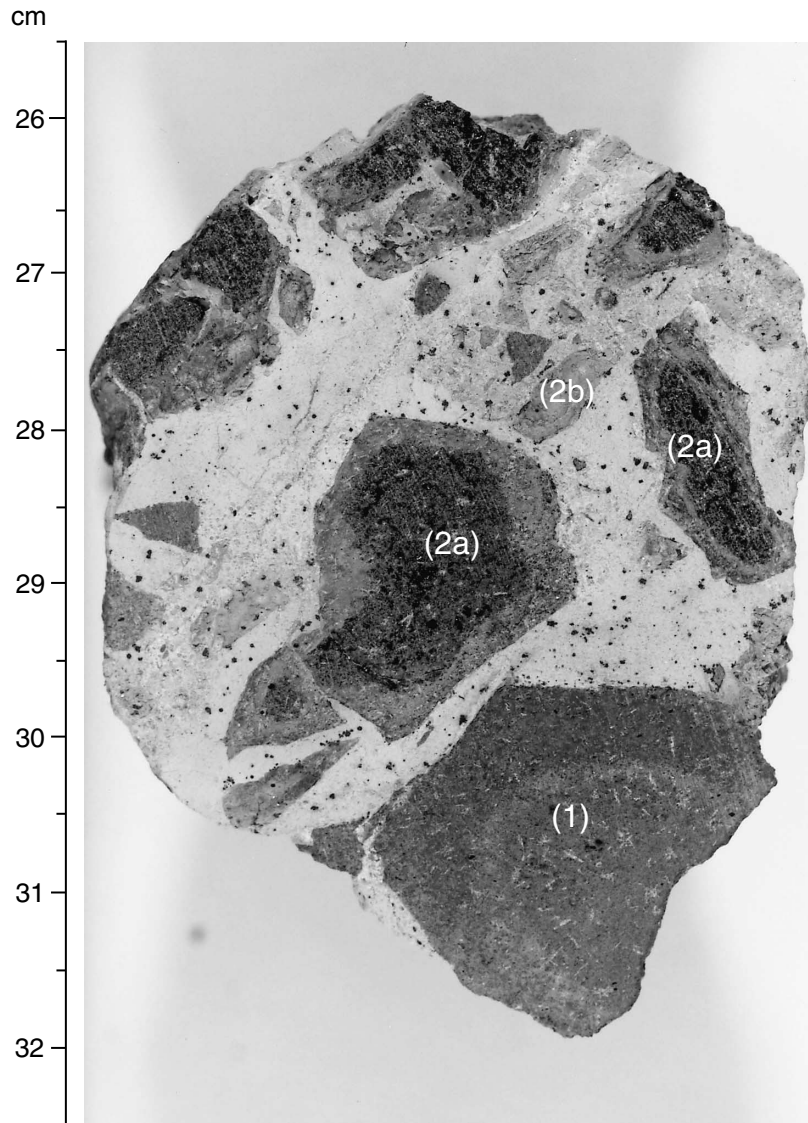


Figure F10. Photograph of interval 187-1163A-11R-1, 90–97 cm, showing calcite-cemented basaltic breccia. The outer margin of the largest basalt clast truncates the alteration halo, indicating that alteration preceded this phase of brecciation.

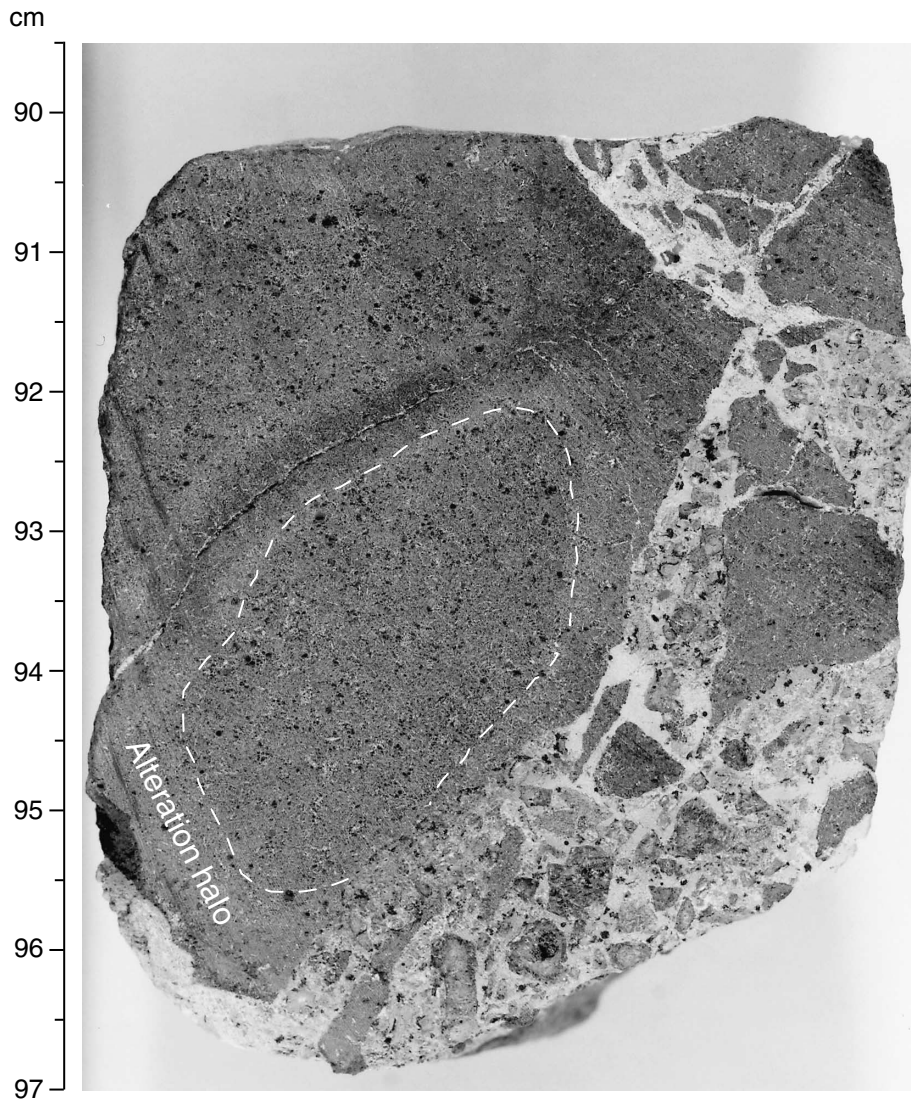


Figure F11. Photograph of interval 187-1163A-3R-2, 1-9 cm, showing a fracture cutting basalt. Note the minor alteration halo along the fracture.

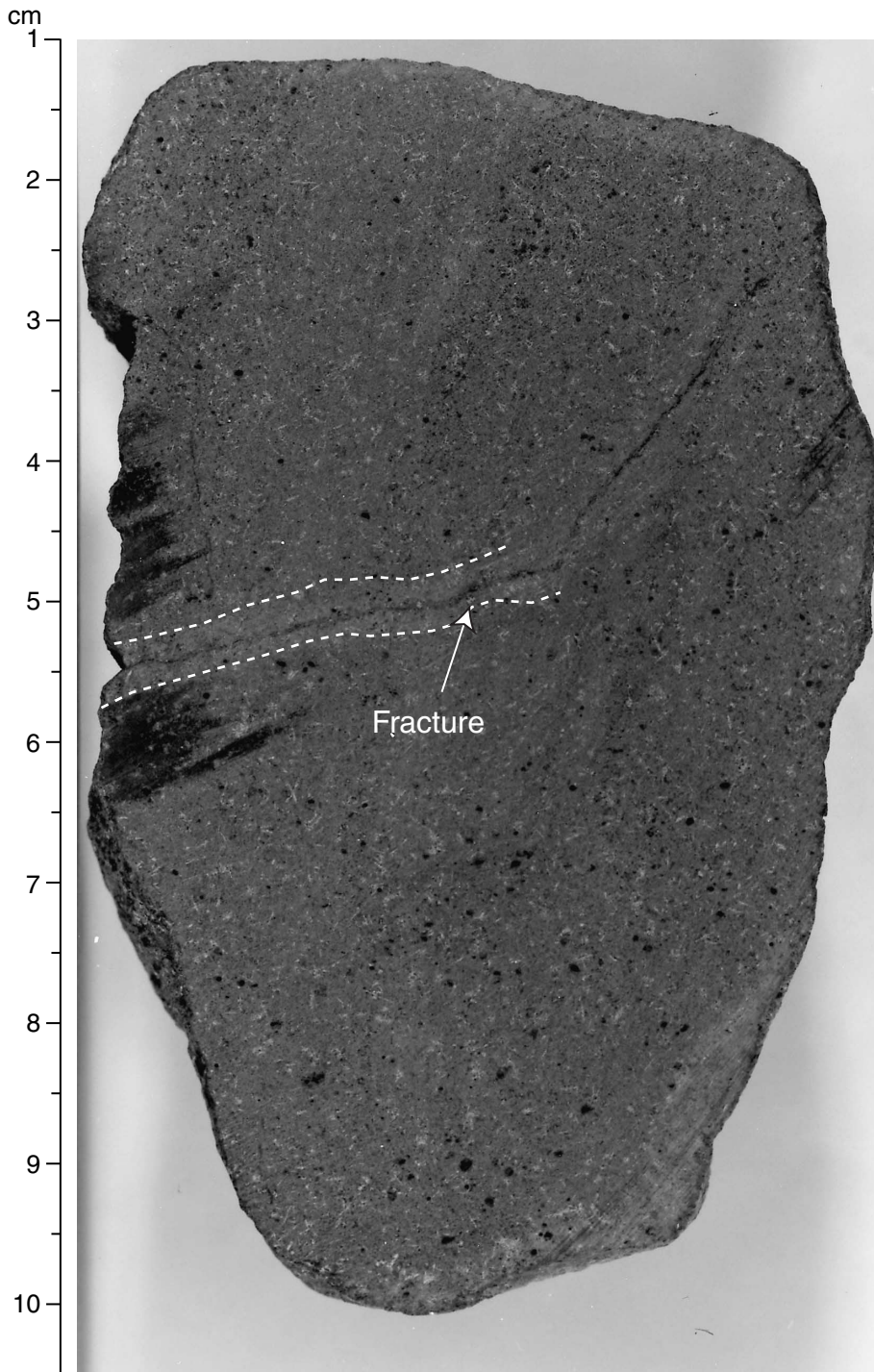


Figure F12. Photograph of interval 187-1163A-9R-1, 97–117 cm, showing a network of calcite veins of varying widths cutting basalt and surrounded by alteration halos.

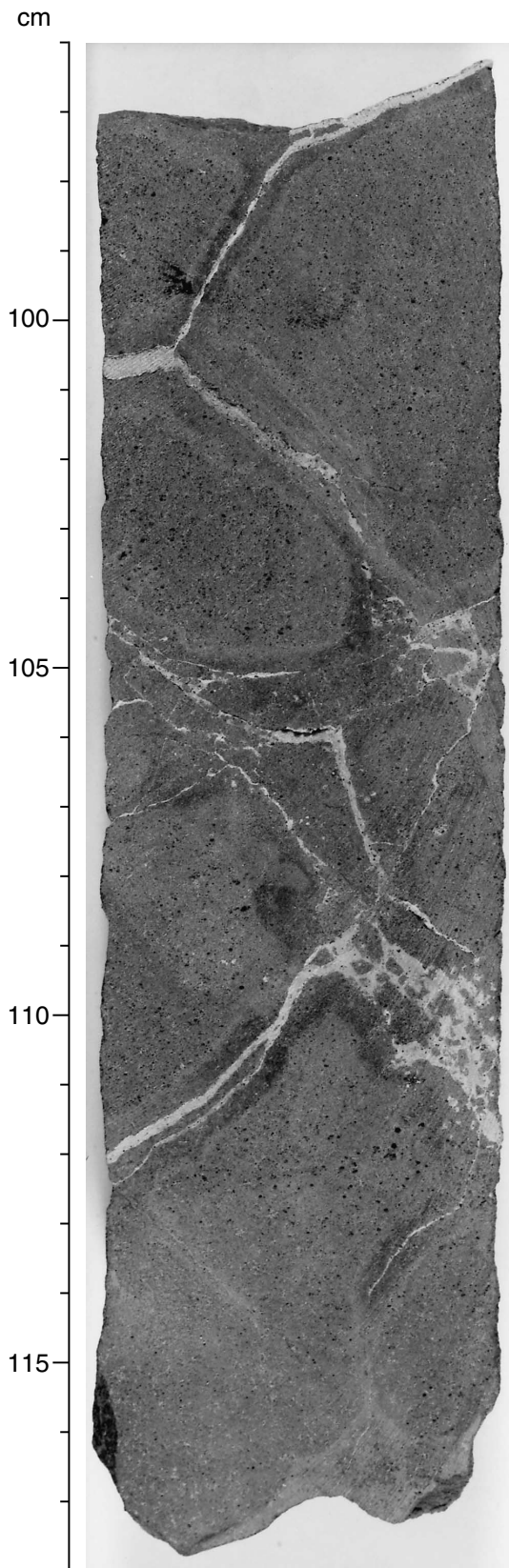


Figure F13. Photograph of interval 187-1163A-10R-1, 41–52 cm, showing carbonate veins surrounded by alteration halos in basalt. Note the lithic clasts in the wider, partially micrite-filled vein in the upper part. Veins in the lower (<44 cm) part are sparry calcite.

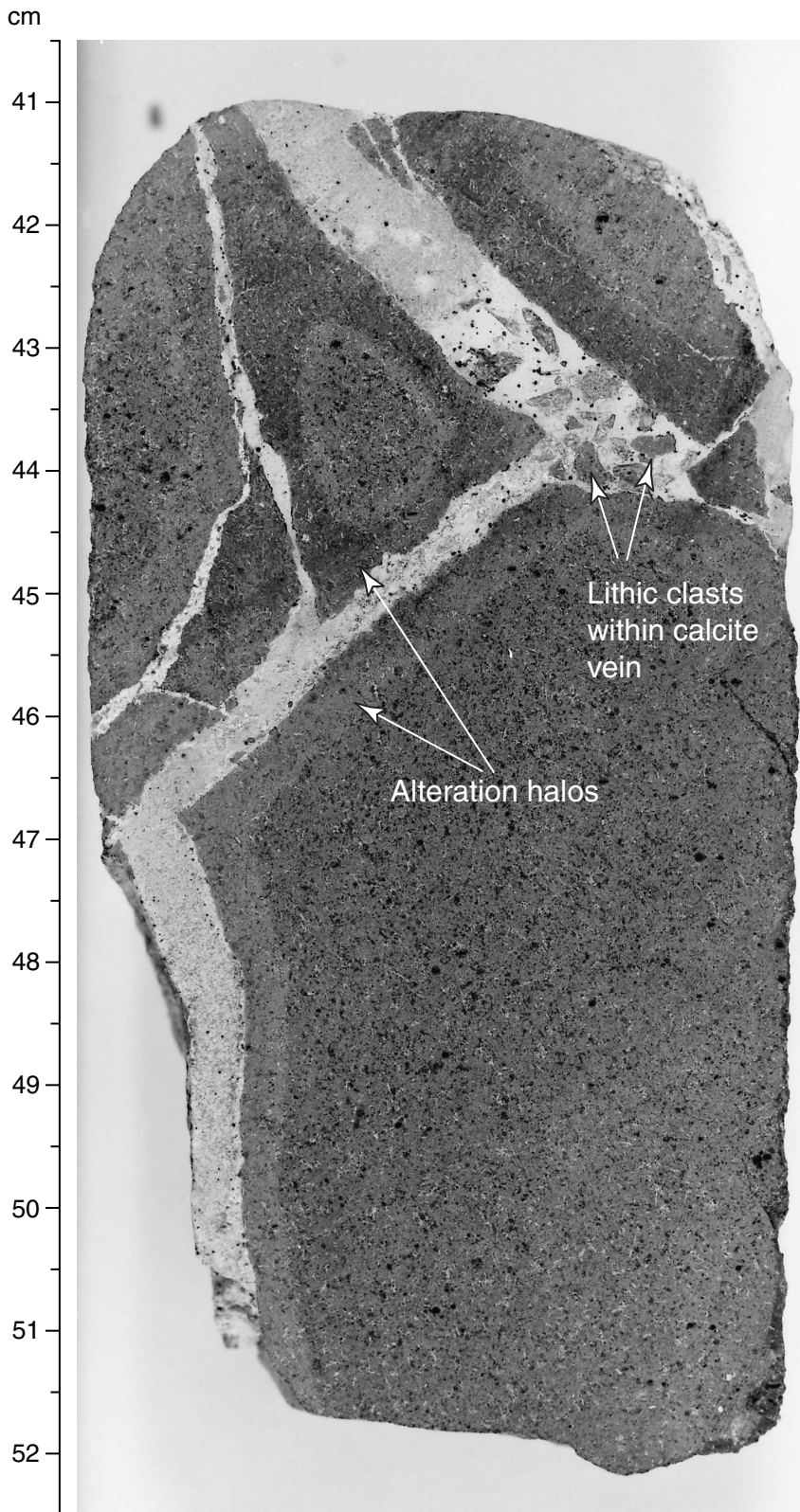
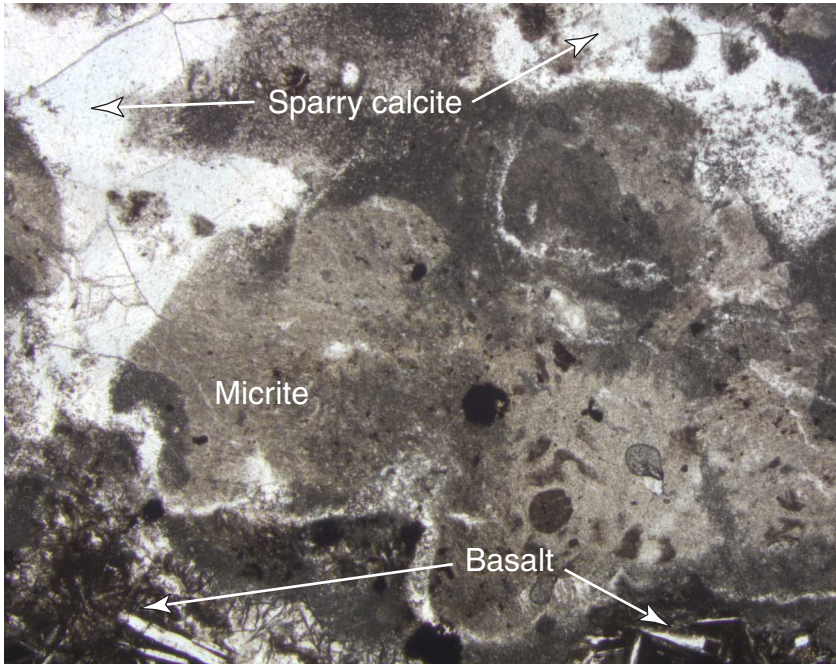


Figure F14. Photomicrograph in plane-polarized light of Sample 187-1163A-3R-1, 63–67 cm (see “[Site 1163 Thin Sections](#),” p. 25), showing a sparry calcite vein cutting micritic calcite and basalt.



2 mm



Figure F15. Photograph of interval 187-1163A-3R-1, 106–114 cm, showing an aphyric basalt piece with alteration halos along the outer margins.

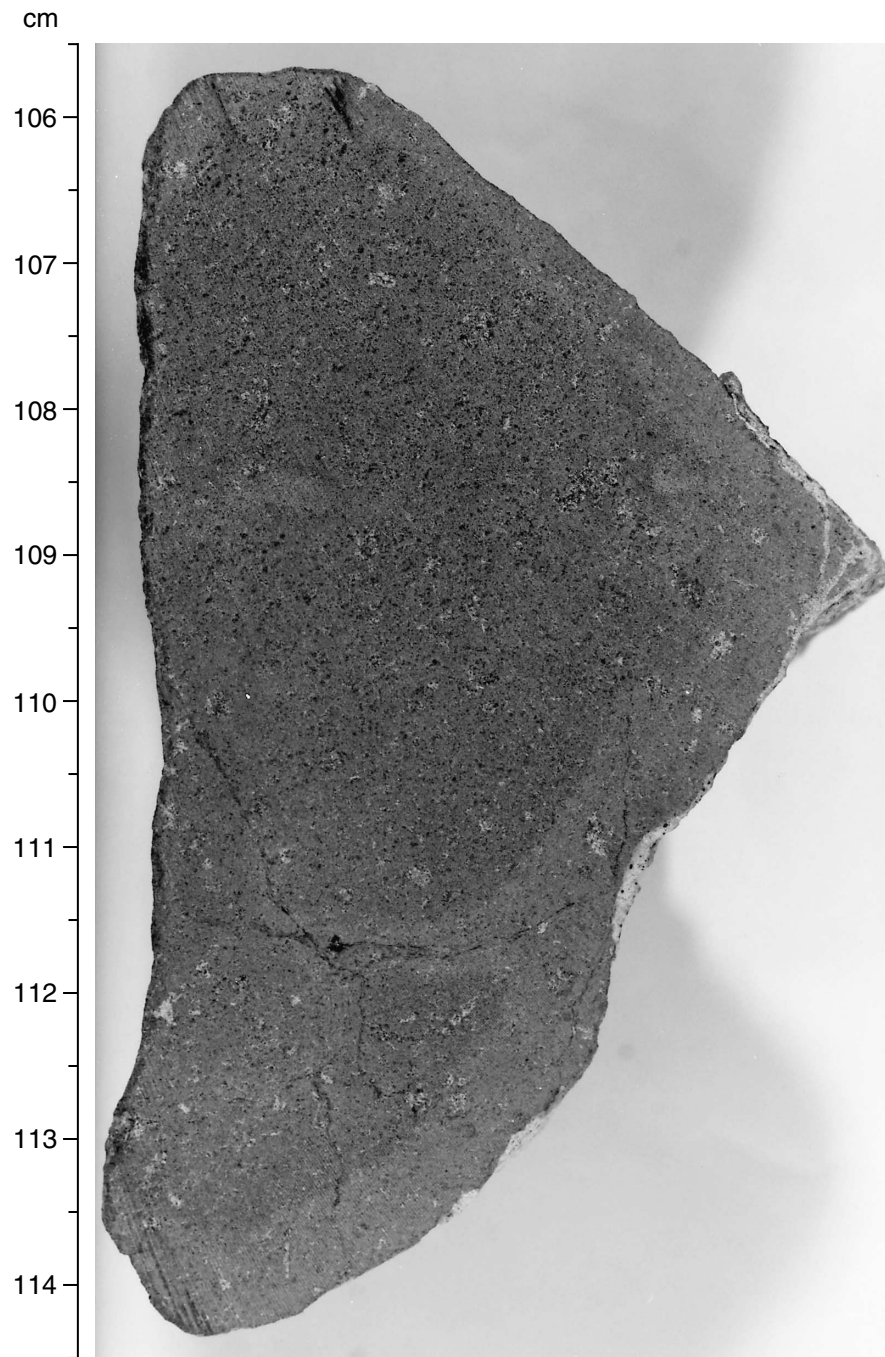


Figure F16. Photograph of contiguous core pieces of basalt cut by veins filled with micritic clay (interval 187-1163A-10R-1, 66–75 cm). Note the alteration halos developed around the veins. Small fragments of basalt and palagonite occur within the micritic clay. Note the reconstruction of drilling-induced fractures.

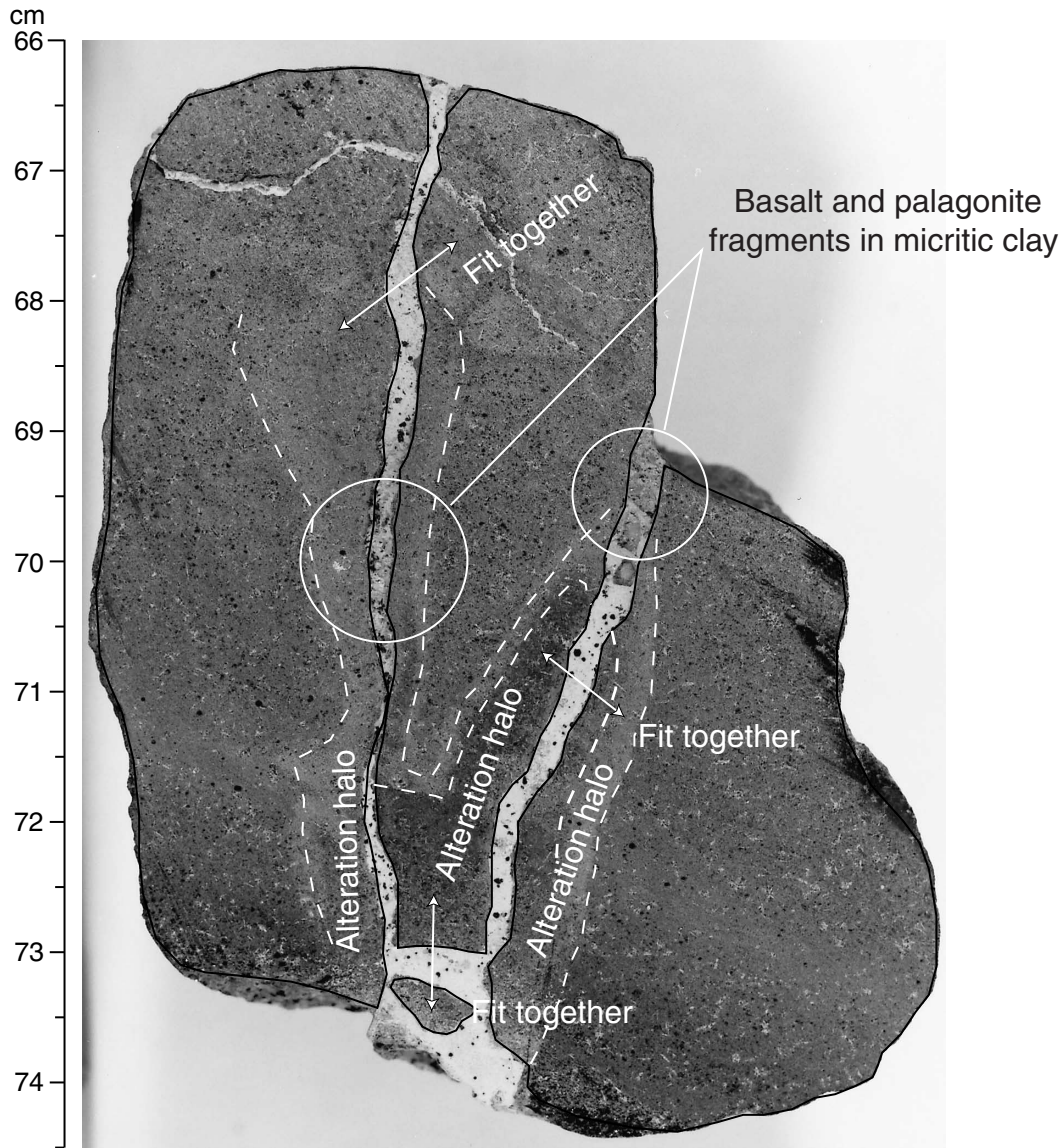


Figure F17. A plot of fracture + vein density (N/m = number per meter of core) calculated for each section from Hole 1163A. The horizontal thick line and associated number represent the average.

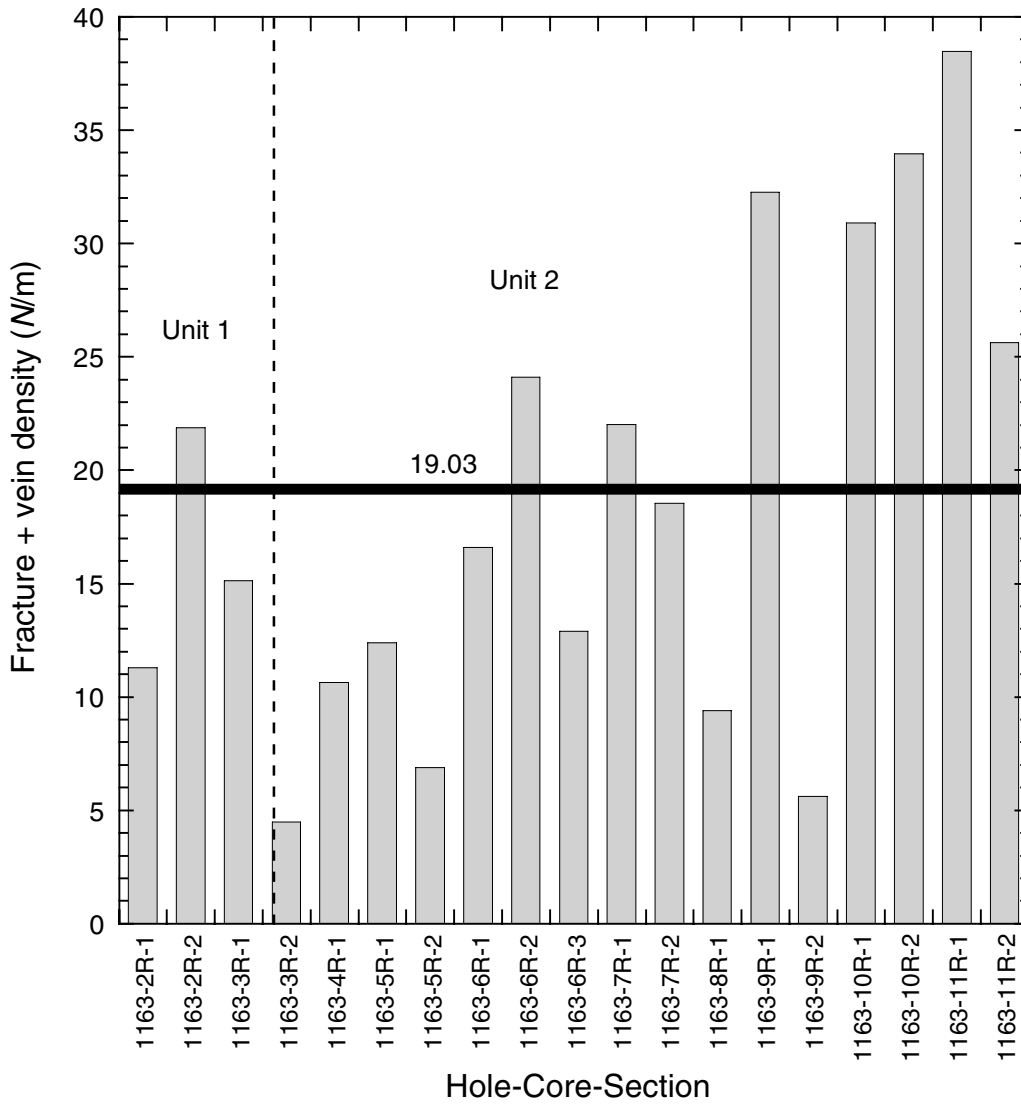


Figure F18. Track chart of the single-channel seismic survey line S11. Crosses = 50-shot intervals for line S11. Site 1163 (solid circle) is near shotpoint 292, ~46 m north of the prospectus site AAD-3b (open circle).

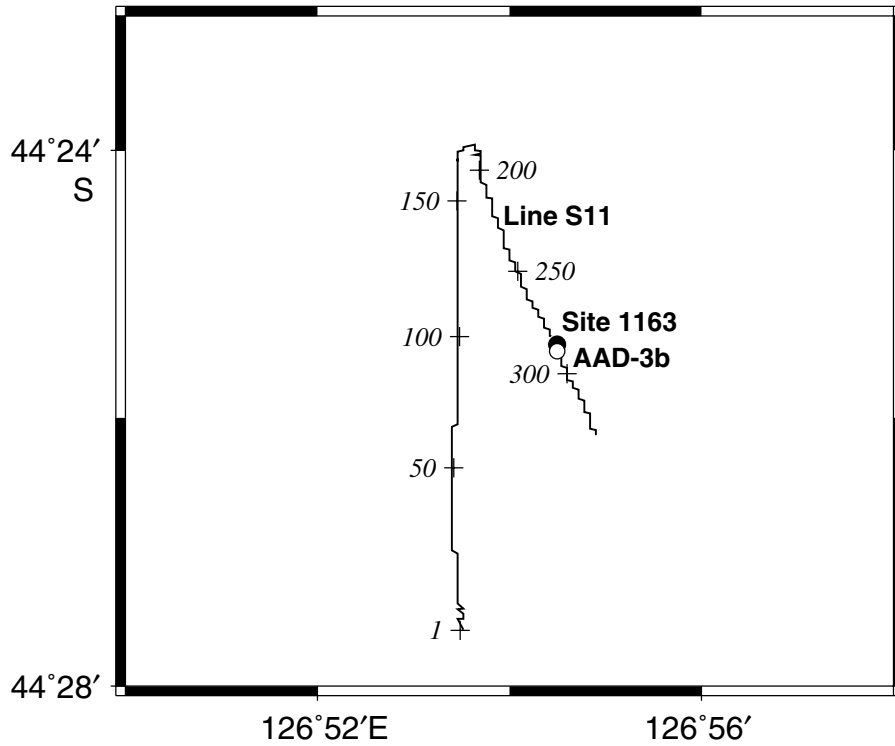
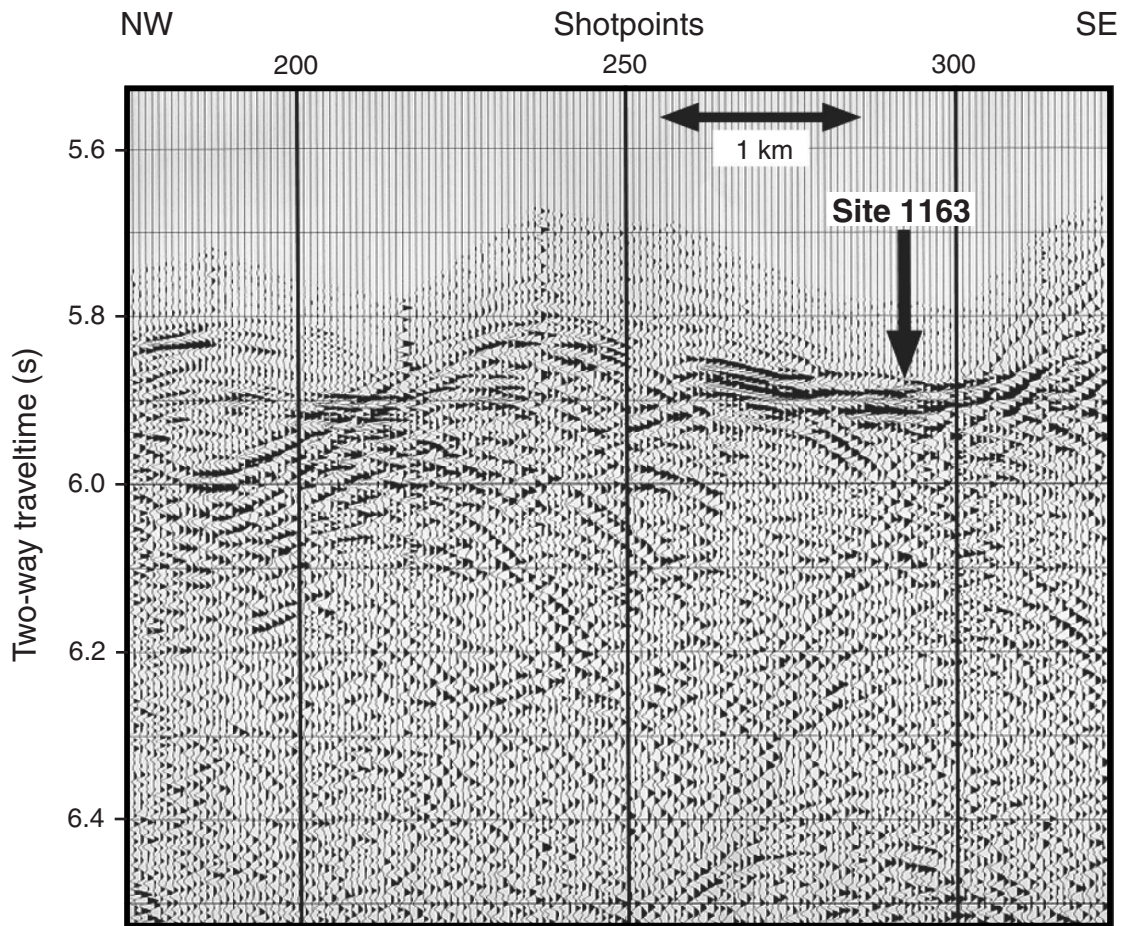


Figure F19. The single-channel seismic profile of line S11 from shotpoints 175 to 322. The heavy arrow marks the position of Site 1163 near shotpoint 292.



Shot interval = 12 s, speed = 5.1 kt, course = 154°

Figure F20. Major element compositions vs. MgO of basalts from Holes 1163A and 1163B compared with glasses from Segment B4. Only the average X-ray fluorescence or ICP-AES analyses reported in Table T3, p. 33, are plotted.

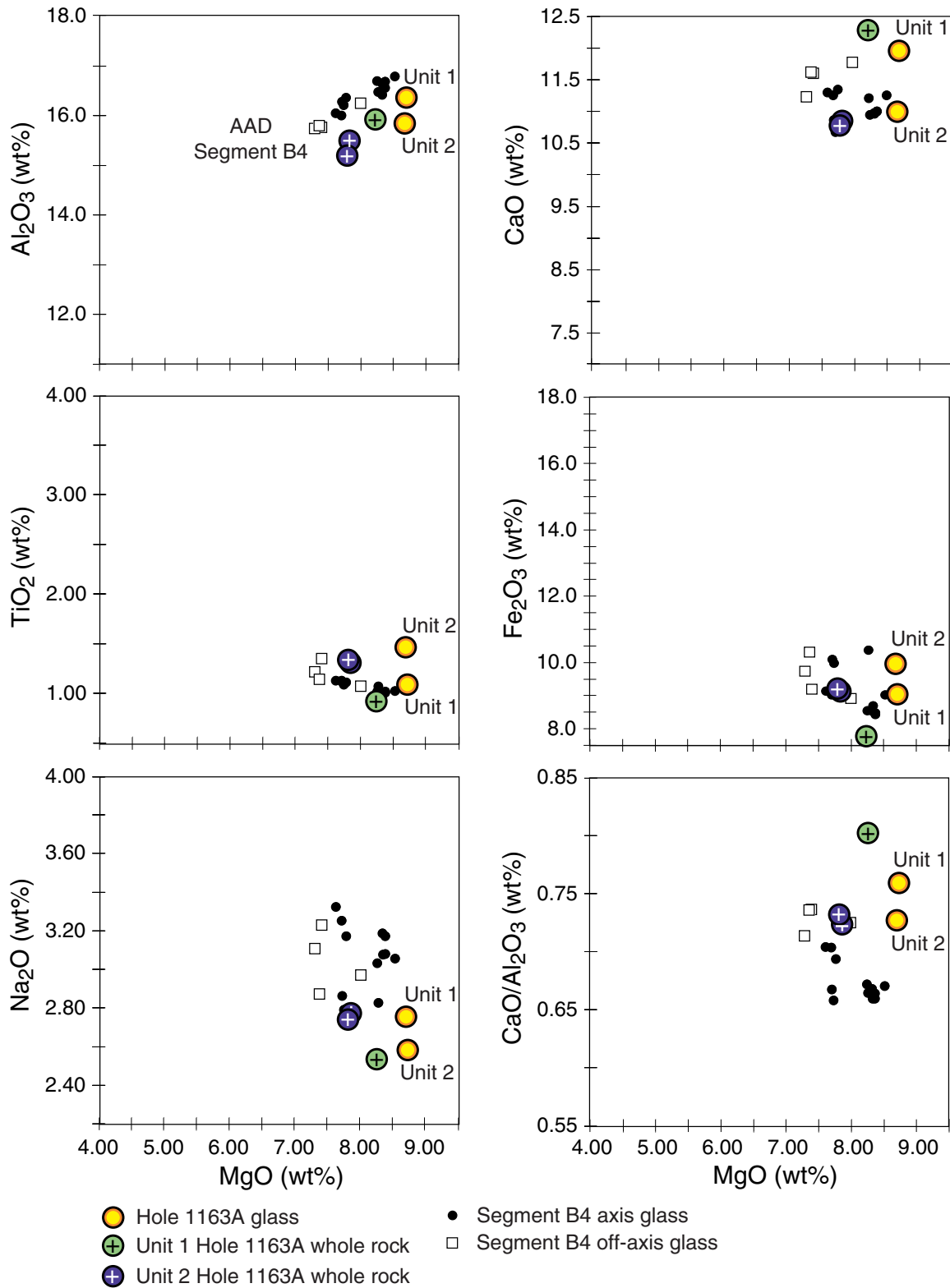


Figure F21. Trace element compositions vs. MgO for Hole 1163A basalts compared with glasses from Segment B4. AAD = Australian Antarctic Discordance.

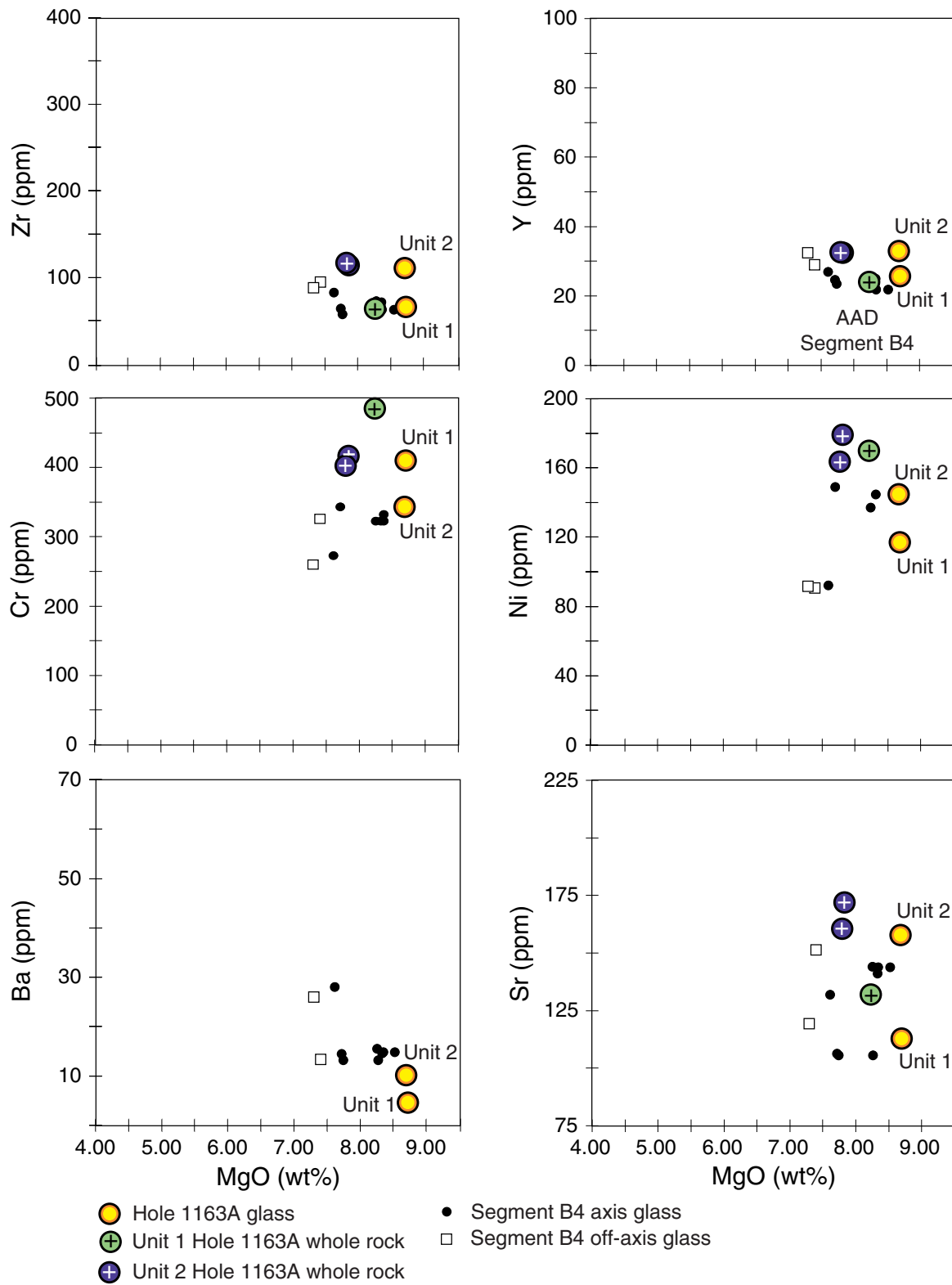


Figure F22. A. Variations of Zr/Ba vs. Ba for Hole 1163A basaltic glass samples compared with Indian- and Pacific-type mid-ocean-ridge basalt (MORB) fields defined by zero-age Southeast Indian Ridge (SEIR) lavas dredged between 123°E and 133°E. TP = Transitional Pacific; PRT = propagating rift tip lavas. **B.** Variations of Na₂O/TiO₂ vs. MgO for Hole 1163A basaltic glass and whole-rock samples compared with Indian- and Pacific-type MORB fields defined by zero-age SEIR lavas dredged between 123°E and 133°E. Dashed line separates Indian- and Pacific-type zero-age SEIR basalt glass.

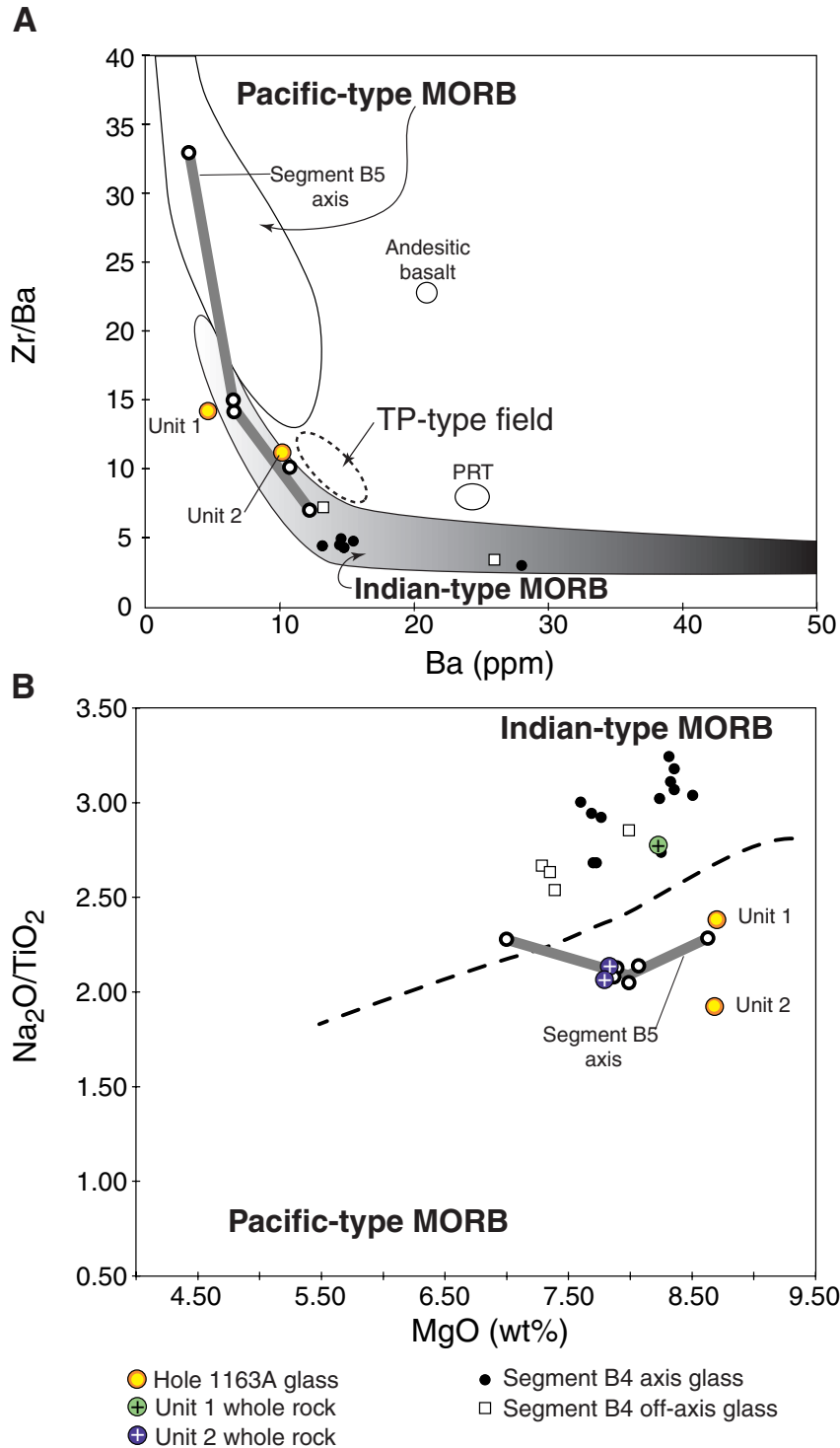


Table T1. Coring summary, Site 1163.

Hole 1163A

Latitude: 44°25.4756'S
 Longitude: 126°54.4978'E
 Time on hole: 0100 hr, 1 Jan 2000–0730 hr, 3 Jan 2000 (54.5 hr)
 Time on site: 0100 hr, 1 Jan 2000–0730 hr, 3 Jan 2000 (54.5 hr)
 Seafloor (drill-pipe measurement from rig floor, mbrf): 4365.4
 Distance between rig floor and sea level (m): 11.4
 Water depth (drill-pipe measurement from sea level, m): 4354.0
 Total depth (from rig floor, mbrf): 4573.5
 Total penetration (mbsf): 208.1
 Total length of cored section (m): 47.1
 Total length of drilled intervals (m): 161.0
 Total core recovered (m): 15.7
 Core recovery (%): 33.3
 Total number of cores: 10
 Total number of drilled cores: 1

Core	Date (Jan 2000)	Ship local time	Depth (mbsf)		Length (m)		Recovery (%)	Comment
			Top	Bottom	Cored	Recovered		
187-1163A-								
1W	1	1515	0.0	161.0	161.0	2.09	N/A	
2R	1	1925	161.0	165.4	4.4	1.44	32.7	Whirl-Pak
3R	1	2240	165.4	171.4	6.0	1.59	26.5	
4R	2	0115	171.4	175.9	4.5	1.11	24.7	
5R	2	0355	175.9	180.8	4.9	1.37	28.0	
6R	2	0725	180.8	185.2	4.4	2.88	65.5	
7R	2	1015	185.2	189.9	4.7	2.03	43.2	
8R	2	1310	189.9	194.1	4.2	0.66	15.7	
9R	2	1555	194.1	199.1	5.0	1.67	33.4	
10R	2	1855	199.1	203.1	4.0	1.30	32.5	
				Cored:	47.1	15.70	33.3	
				Drilled:	161.0			
				Total:	208.1			

Notes: N/A = not applicable. This table is also available in [ASCII format](#).

Table T2. Rock samples incubated for enrichment cultures and prepared for DNA analysis and electron microscope studies and microspheres evaluated for contamination studies.

Core	Depth (mbsf)	Sample type	Enrichment cultures				DNA analysis		SEM/TEM samples	Microspheres [†]	
			Anaerobic	Aerobic	Microcosm*	High pressure	Wash	Fixed	Air dried	Exterior	Interior
187-1163A-											
2R	161.0-165.4	Chilled margin	7	3	1 Fe/S	X	X	X	X	Yes	Yes
4R	171.4-175.9	Chilled margin	7	3			X	X	X		
8R	189.9-194.1	Breccia	7	3			X	X	X		
10R	199.1-203.1	Fine-grained basalt	8	3			X	X	X		

Notes: * = microcosm for iron and sulfur (Fe/S) or manganese redox cycles; SEM = scanning electron microscope; TEM = transmission electron microscopy; † = contamination test; X= sample prepared on board. This table is also available in [ASCII format](#).

Table T3. Glass and whole-rock major and trace element compositions of basalts, Site 1163.

Core, section:	Hole 1163A											
	1W-CC	1W-CC	1W-CC	1W-CC	2R-2	2R-2	3R-2	3R-2	8R-1	8R-1	10R-1	10R-1
Interval (cm):	19-21	19-21	19-21	19-21	67-70	67-70	0-4	0-4	41-43	41-43	116-120	116-120
Depth (mbsf):	2.07	2.07	2.07	2.07	163.17	163.17	166.85	166.85	190.31	190.31	200.26	200.26
Piece:	1	1	1	1	10b	10b	1	1	6	6	13	13
Unit:	1	1	1	1	1	1	2	2	2	2	2	2
Analysis:	ICP	ICP	ICP	ICP	XRF	XRF	XRF	XRF	ICP	ICP	XRF	XRF
Rock type:	Glass	Glass	Glass	Glass	Moderately plagioclase- olivine phyric basalt		Aphyric basalt		Glass	Glass	Aphyric basalt	
Major element (wt%)												
SiO ₂	51.07	50.14	52.30	52.01	49.28	49.34	48.78	49.37	51.07	50.14	48.75	49.93
TiO ₂	1.12	1.05	1.10	1.07	0.90	0.93	1.29	1.31	1.12	1.05	1.31	1.35
Al ₂ O ₃	16.33	16.10	16.76	16.15	15.86	15.93	15.34	15.59	16.33	16.10	14.96	15.38
Fe ₂ O ₃	9.32	8.90	8.95	8.96	7.78	7.77	9.03	9.22	9.32	8.90	9.03	9.39
MnO	0.17	0.15	0.15	0.15	0.12	0.12	0.14	0.14	0.17	0.15	0.13	0.14
MgO	9.05	8.45	8.73	8.59	8.22	8.24	7.80	7.87	9.05	8.45	7.68	7.91
CaO	12.71	12.21	12.48	12.28	12.79	12.76	11.13	11.29	12.71	12.21	11.01	11.24
Na ₂ O	2.58	2.57	2.53	2.67	2.52	2.56	2.72	2.83	2.58	2.57	2.70	2.79
K ₂ O	0.08	0.07	0.08	0.08	0.17	0.17	0.23	0.24	0.08	0.07	0.26	0.26
P ₂ O ₅	0.11	0.10	0.10	0.11	0.08	0.08	0.16	0.17	0.11	0.10	0.16	0.17
LOI					0.64	0.64	1.24	1.24			0.79	0.79
CO ₂												
H ₂ O												
Total:	102.52	99.73	103.19	102.06	97.72	97.90	96.62	98.03	102.52	99.73	95.99	98.56
Trace element (ppm)												
Nb					3		6				5	
Zr	66	66	67	71	65		116		109	115	118	
Y	26	25	24	27	24		32		33	32	32	
Sr	113	114	116	109	132		172		156	160	161	
Rb					2		2				2	
Zn					64		78				76	
Cu					71		62				59	
Ni	121	115	122	112	170		179		148	142	164	
Cr	425	397	418	402	486		417		366	321	403	
V					204		232				241	
Ce					13		29				27	
Ba	5	4	6	6					11	10		
Sc	35	34	33	36					34	34		

Notes: CC = core catcher; LOI = loss on ignition. This table is also available in [ASCII format](#).